Progress In Electromagnetics Research C, Vol. 7, 13–24, 2009

EFFECTS OF SOIL PHYSICAL PROPERTIES ON LAND-MINES DETECTION USING MICROSTRIP ANTENNA AS A SENSOR

S. H. Zainud-Deen, M. E. Badr, E. M. Ali, K. H. Awadalla and H. A. Sharshar

Faculty of Electronic Engineering
Menoufia University
Menouf, Egypt

Abstract—The effect of soil properties on landmines detection using Microstrip antenna with corrugated ground between the two microstrip elements as a sensor has been investigated. The effect of the electrical properties of the soil as well as the shape of the soil surface on the detection capability of the sensor is studied. The Finite-Difference Time-Domain (FDTD) has been used to simulate the sensor for landmines detection.

1. INTRODUCTION

Landmines are a humanitarian challenge because they indiscriminately kill and maim civilians. The variety of environmental conditions in which mines can be found is enormous. Minefields are not only neat ordered rows of mines in flat deserts but can also be found among the debris of burnt-out buildings and post-conflict urban and rural environments. Mine detection equipment has to be designed to work in a wide range of physical environments. Detection equipment must be able to operate in climatic conditions, which range from arid desert, hillside screen to overgrown jungle. Rain, dust, humidity and solar isolation must all be considered in the design and operation of equipment [1–5]. The mines encountered today come in a plethora of size and material and are buried at various depths, in various types of soil land under various conditions. A separated-aperture sensor, which consists of two parallel dipole antennas housed in corner reflectors that are separated by a metallic septum, has been investigated in [6–8]. Using the mutual coupling behavior between the two dipoles

Corresponding author: S. H. Zainud-Deen (anssaber@yahoo.com).

the presence of a buried target is determined. Recently two patch antennas have been proposed for the detection of buried land mines [9–12]. The two microstrip antenna with corrugated ground plane as a sensor for landmines detection has been investigated. The corrugated ground between the two microstrip elements has the advantage of high surface impedance which leads to the reduction of the mutual coupling between the two microstrip antenna, and hence increasing the detection capability of the sensor [11].

The velocity of propagation is primarily governed by the relative permittivity of the material, which depends primarily upon its water content. Water has a relative permittivity of ≈ 80, while the solid constituents of most soils and man-made materials have, when dry, a relative dielectric constant ε_r in the range 2 to 9, the measured value ε_r for soil and building materials lie mainly between the range 4 to 40. A reflection occurs when the emitted signal encounters a surface between two electrically different materials. The intensity and direction of the reflection depend on two factors: The roughness of the surface and the electric property of the medium material. A rough surface reflects the incoming radiation in a diffused manner, while smooth surface tends to reflect at the same angle as the incoming radiation with respect to the surface normal. The electric property of the medium affects the direction and intensity of the reflection [5].

The previous work by the authors [10–12] considered only the case of a soil with smooth surface. In this paper, the detection capability of the two parallel microstrip antenna with corrugated ground between the elements is investigated. A soil with rough ground surface, which is close to the practical case, containing a buried target is considered for the first time. Also, a soil consists of two layers with different electrical properties is investigated. A finite-difference time-domain (FDTD) technique is developed by the authors to simulate the problem of landmines detection. A brief analysis of FDTD technique is shown in Section 2, Section 3 concludes the results, and the conclusions are given in Section 4.

2. FDTD TECHNIQUE

The FDTD technique is an approach that solves the Maxwell's equations by a proper discretization in both space and time domains. The differential form of Maxwell's equations can be written as:

$$\nabla \times E = -\mu \frac{\delta H}{\delta t} - \sigma^* H \tag{1}$$

$$\nabla \times H = \varepsilon \frac{\delta E}{\delta t} + \sigma E \tag{2}$$

where

E: Electric field intensity (Volt/meter),

H: Magnetic field intensity (Ampere/meter)

σ : Electric conductivity (Siemens/meter),

σ^*: Equivalent magnetic loss (Ohms/meter)

ε : Electrical permittivity (Farad/meter),

μ: Magnetic permeability (Henry/meter)

Yee [13] discretized the space of the problem to small cubical cells and for each cell he locates the six field components to match the curl equations. The electric field vectors are located at the center of the cube edges and parallel to the cube edges, while the magnetic field vectors are located at the center of the cube faces and normal to the cube faces. The partial derivatives with respect to the space and time can be approximated using the central difference approximation. The six update equations of the magnetic and electric field components can be obtained as in [9].

In this work, the FDTD method with 10-cell thick for uniaxial perfect matched layer (UPML) is used to simulated the far field condition. The space steps used in simulation are $\Delta x = 1.7308$ mm, $\Delta y = 1.6014$ mm, and $\Delta z = 0.9415$ mm. The time step, Δt, is selected to satisfy 0.9 of Courant limit [14]. A Gaussian pulse with $T = 66$ ps is used as the excitation pulse. More details about the FDTD technique can be found in [14, 15].

3. NUMERICAL RESULTS

FDTD simulation has been carried out to show the detection capability of the sensor to detect a target buried inside soil. Different ground surface shapes and soils with different electrical properties are considered. The sensor consists of two microstrip patch with corrugated ground plane between the two patches as shown in Fig. 1. Each patch has length $L = 11.690$ cm, patch width $W = 18.865$ cm, substrate thickness $d = 0.283$ cm, the feed position of $x = 3.362$ cm, $y = 9.432$ cm and the spacing between the two patches is $\lambda_o/2 = 18.987$ cm. The resonance frequency $f_o = 790$ MHz. The corrugated ground plane is specified by slot width $w_s = 0.1\lambda_o = 3.7974$ cm, the ridge thickness $w_c = 0.03\lambda_o = 1.139$ cm, while the depth is $h = \lambda_o/4 = 9.4935$ cm [11]. One of the patches is considered as the transmitting antenna while the other patch is considered as the receiving antenna. The sensor is located in air at height $h_2 = 2.8$ cm from the surface of the ground, while the metallic target is buried in

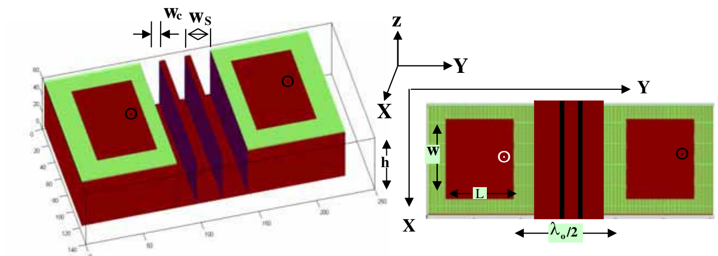

(a) 3D view (b) Top view

Figure 1. 3D geometry and top view of two element coaxial fed with corrugated ground surface, at $f_o = 790\,\text{MHz}$, $W = 18.86\,\text{cm}$, $L = 11.69\,\text{cm}$, $d = 0.1588\,\text{cm}$, feed position at $x = 3.362\,\text{cm}$, $y = 9.43\,\text{cm}$ slot width (groove width) $w_s = 0.1\lambda_o$, the ridge thickness $w_c = 0.03\lambda_o$ and the corrugation depth $h = \lambda_o/4$.

the soil at depth $d_2 = 7.6\,\text{cm}$. The geometry of the problem is shown in Fig. 2. When the sensor is moved over an empty soil, a small portion of the signal will be reflected from the surface of the ground back to the receiving antenna, causing a small mutual coupling between the transmitting and the receiving antennas. When the sensor is moved over a soil containing a buried target, the target reflects a portion of the radiated signal by the transmitting antenna back to the receiving antenna. Different types of soil have been investigated using FDTD simulations. The simulation includes the sensor construction, location in air, ground surface shape, the soil properties and the buried target.

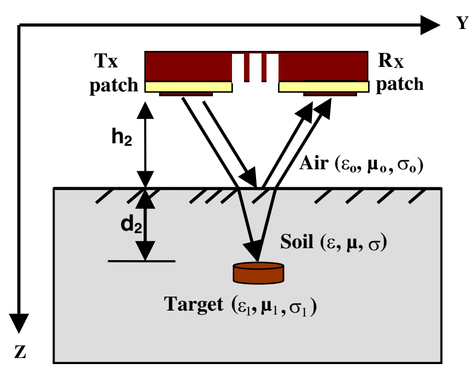

Figure 2. Geometry of the whole problem for landmines detection, the domain includes the sensor in air at certain height (h_2) and the target buried at depth (d_2).

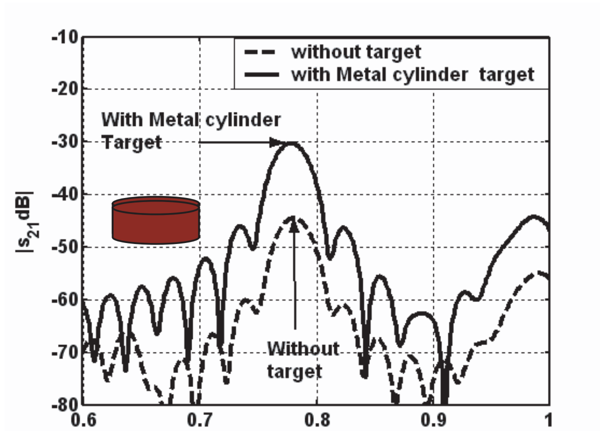

Figure 3. $|S_{21}|$ of sensor to detect metal cylinder target buried in soil with $\varepsilon_r = 2.9$ at depth $d_2 = 7.6\,\text{cm}$ and $h_2 = 2.8\,\text{cm}$.

3.1. Smooth Ground Surface

In this case, three examples are considered:

3.1.1. Example (1). One Layer Soil

The sensor is placed over soil with smooth ground surface. The soil tends to reflect the signal at the same angle as the incoming radiation with respect to the surface normal. The soil is described as "loamy soil" with electrical properties of ε_r=2.9, $\mu_r = 1.0$, and $\sigma = 0.02\,\text{S/m}$ [5]. The buried target in the soil is circular metal target contains TNT materials. The target with diameter=11.0 cm, height=5.5 cm, and $\sigma = 5.8 \times 10^7\,\text{S/m}$ is used. Fig. 3 shows the calculated mutual coupling, $|S_{21}|$ between the two antennas versus the operating frequency, without and with metallic circular target. The difference between the two cases is 14.5 dB.

In the second case of study the soil is described as "red clay" with electrical properties of $\varepsilon_r = 8.1$, $\mu_r = 1.0$, and $\sigma = 0.038\,\text{S/m}$ [5]. Fig. 4 shows the calculated mutual coupling, $|S_{21}|$ as a function of the operating frequency, the difference between the two cases is about 12.6 dB. It is noted that the amplitudes of $|S_{21}|$ are depending on the soil properties for the same target and ground surface.

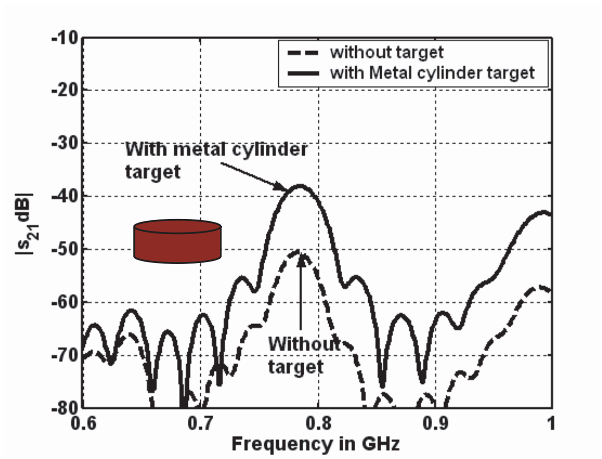

Figure 4. $|S_{21}|$ of sensor to detect metal cylinder target buried in soil with $\varepsilon_r = 8.1$ at depth $d_2 = 7.6$ cm and $h_2 = 2.8$ cm.

3.1.2. Example (2). Two Layer Soil

The soil consists of two layers with different electrical properties. The first layer is described as "loamy dry soil" with electrical properties of $\varepsilon_{r1} = 2.9$, $\mu_{r1} = 1.0$, and $\sigma_1 = 0.1$ S/m and with thickness=5.157 cm, the second layer of soil is described as "loamy wet soil" with an electrical properties $\varepsilon_{r2} = 5.0$, $\mu_{r2} = 1.0$, and $\sigma_2 = 0.1$ S/m as shown in Fig. 5. The target is locating in the second layer. Fig. 6 depicts the

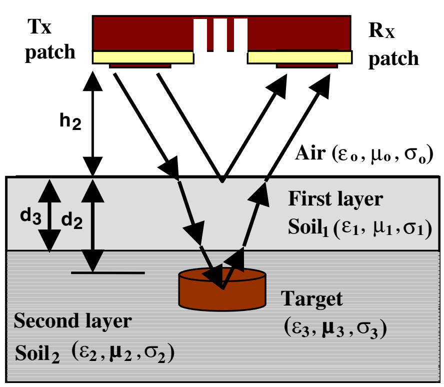

Figure 5. Geometry of the problem for landmine detection including two different soil properties.

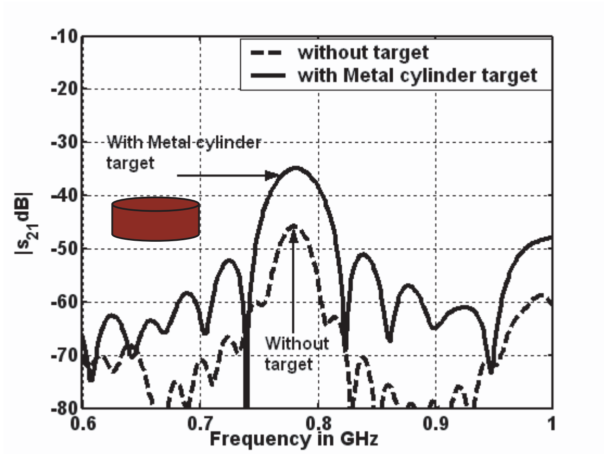

Figure 6. $|S_{21}|$ of sensor to detect metal cylinder target buried in two different soil, dry soil $\varepsilon_r = 2.9$, with thickness $d_3 = 5.157$ mm and wet soil $\varepsilon_r = 5$ at $d_2 = 7.6$ cm.

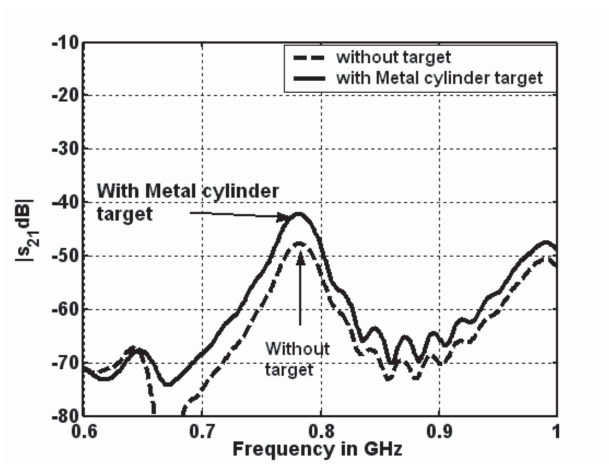

Figure 7. $|S_{21}|$ of sensor to detect metal cylinder target buried in two different soil, dry soil $\varepsilon_r = 8.1$ with thickness $d_3 = 5.157$ mm and wet soil $\varepsilon_r = 15$ at $d_2 = 7.6$ cm.

calculated mutual coupling, $|S_{21}|$, resulting in the two cases of without and with metallic circular target. The difference between the two cases is about 10.88 dB.

In the second case the soil consists of two layers. The first layer is described as "red clay dry soil" with electrical properties of $\varepsilon_{r1} = 8.1$, $\mu_{r1} = 1.0$, and $\sigma_1 = 0.038\,\mathrm{S/m}$ and with thickness=5.157 cm, the second layer of soil is "red clay wet soil" with electrical properties ε_{r2}=15, $\mu_{r2} = 1.0$, and $\sigma_2 = 0.01\,\mathrm{S/m}$. Fig. 7 shows the calculated mutual coupling, $|S_{21}|$ as a function of the operating frequency, the difference between the two cases (without and with target) is 5.53 dB. The detection capability of the sensor in this case has been decreased due to high electrical permittivity of the second soil layer.

In the last case, the first layer of soil is described as "red clay wet soil" with electrical properties $\varepsilon_{r1} = 15$, $\mu_{r1} = 1.0$, and $\sigma_1 = 0.01\,\mathrm{S/m}$ and with thickness=5.157 cm, the second layer of soil is "red clay dry soil" with electrical properties of $\varepsilon_{r2} = 8.1$, $\mu_{r2} = 1.0$, and $\sigma_2 = 0.038\,\mathrm{S/m}$. Fig. 8 shows the calculated mutual coupling, $|S_{21}|$ as a function of the operating frequency, the difference between the two cases (without and with target) is about 11.85 dB.

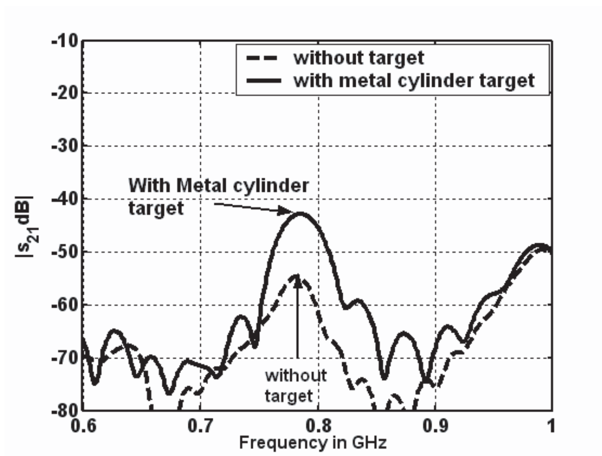

Figure 8. $|S_{21}|$ of sensor to detect metal cylinder target buried in two different soil, wet soil $\varepsilon_r = 15$ and dry soil with $\varepsilon_r = 8.1$ at $d_2 = 7.6\,\mathrm{cm}$.

It is clear that the wet soil has more effect on the target detection. It decreases the possibility of detecting the buried object by decreasing the difference mutual coupling between the two antennas in case of without and with target.

3.2. Rough Ground Surface

In this case two examples are considered:

3.2.1. Example (1). Rough Ground with Hemispherical Shape

A rough ground surface is represented as a series of regular hemispheres. Each hemisphere with radius 3 cm and spacing between two spheres is 9 cm as shown in Fig. 9. A rough ground surface tends to reflect the incoming radiation in a diffused manner. The soil is described as "loamy dry soil". The calculated mutual coupling $|S_{21}|$ as a function of the operating frequency is shown in Fig. 10 in case of without and with metallic circular target. The difference between the two cases is about 12.78 dB.

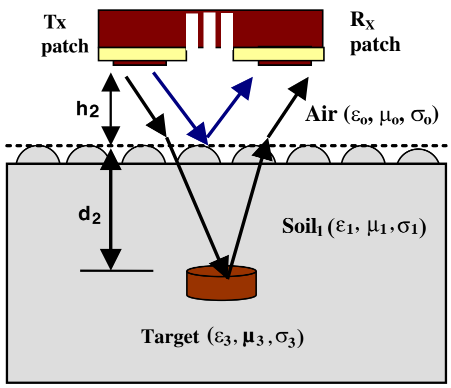

Figure 9. Geometry of the problem for landmine detection in case of a soil with rough surface in the shape of hemisphere with radius 3 cm.

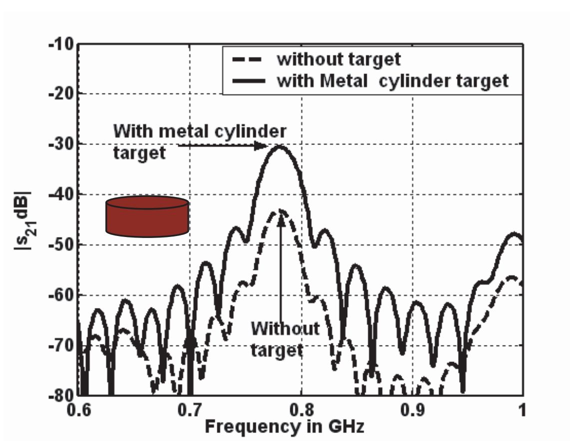

Figure 10. $|S_{21}|$ of sensor to detect metal cylinder target buried in a soil with rough surface modeled as hemisphere, $\varepsilon_r = 2.9$ at $d_2 = 7.6$ cm and sensor height $h_2 = 2.8$ cm.

3.2.2. Example (2). Rough Ground with Staircase Shape

The rough ground surface is modeled as a staircase ground surface; the soil is described as "loamy dry soil" shown in Fig. 11. In this case the depth of the target is $d_3 = 3\,\text{cm}$. The calculated mutual coupling, $|S_{21}|$ as a function of the operating frequency shown in Fig. 12. The difference between the two cases (without and with target) is about 13.1 dB. Table 1 shows comparison of the mutual coupling factor $|S_{21}|$ for the cases of smooth ground surface and rough ground surfaces in

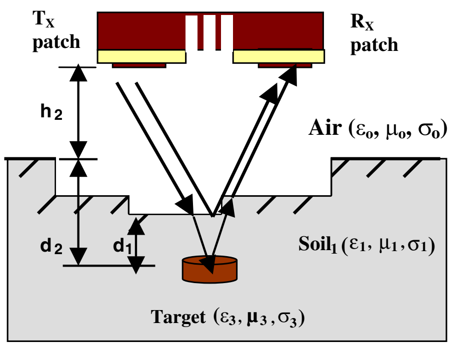

Figure 11. Geometry of the problem for landmine detection in case of a soil with rough surface in.

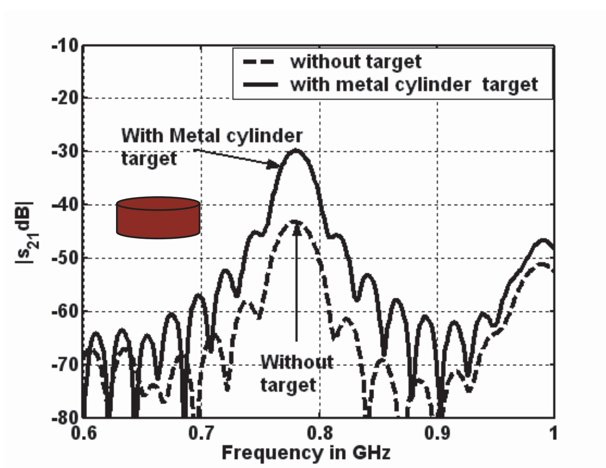

Figure 12. $|S_{21}|$ of Sensor to detect metal cylinder target buried in a soil with rough surface modeled as a staircase surface the soil have $\varepsilon_r = 2.9$ at $d_1 = 3\,\text{cm}$, $d_2 = 7.6\,\text{cm}$ and $h_2 = 2.8\,\text{cm}$.

both cases of without and with target. The possibility of detecting the buried object is decreased as the ground surface is coming rough compared with smooth ground. The difference between the mutual coupling $|S_{21}|$ in case of without and with target is decreased compared with the case of smooth ground.

Table 1 shows the comparison of mutual coupling factor $|S_{21}|$ over different ground surface shapes.

$\lvert S_{21}\rvert$ of Smooth ground			$\lvert S_{21}\rvert$ of Rough Ground (Hemispherical)			$\lvert S_{21}\rvert$ of Rough Ground (Staircases)		
Without target	With Target	The Difference	Without target	With Target	The difference	Without Target	With target	The difference.
-44.5	-30.	14.5	-43.18	-30.4	12.78	-44.9	31.8	13.1

4. CONCLUSION

FDTD technique has been used to simulate the effect of soil properties on landmines detection, using microstrip antennas with corrugated ground surface as a sensor. The effects of varying the shape of the ground surface as well as the electrical properties limit the detection process. The FDTD simulation has been used to simulate the different types of soil shape with different soil properties and the detection capability of the sensor. It has been shown that the amount of scattered signal due the presence of the target is based on the type of the soil, changing of the soil surface, the sensor height or the target depth.

REFERENCES

1. Boutros-Ghali, B., *The Land Mine Crisis*, Foreign Affairs, Vol. 73, 8–13, Sep./Oct. 1994.
2. http://www.un.org/issues/gallery/mines/aboutmines.html, Mines: A Globle Crisis.
3. Benini, A., L. H. Moulton, and C. E. Conley, "Landmines and local community adaptation," *Journal of Contingencies and Crisis Management*, Vol. 10, No. 2, 82–94, 2002.
4. Huang, Q.-J. and K. Nonami, "Humanitarian mine detecting six-legged walking robot and hybrid neuro walking control with position/force control," *Mechatronics*, Vol. 13, 773–790, 2003.
5. Daniels, D. J., *Ground Penetrating Radar*, 2nd Edition, Institution of Electrical Engineer, London, UK, 2004.
6. Bourgeois, J. M. and G. S. Smith, "A full electromagnetic simulation of a ground penetrating radar: Theory and

experiment," *IEEE AP-S. Int. Symp. Dig.*, Vol. 32, 1442–1445, Jun. 1994.

7. Bourgeois, J. M. and G. S. Smith, "A complete electromagnetic simulation of a ground penetrating radar for mine detection: Theory and experiment," *IEEE AP-S. Int. Symp. Dig.*, Vol. 35, 986–989, Jun. 1997.
8. Bourgeois, J. M. and G. S. Smith, "A complete electromagnetic simulation of the separated-aperture sensor for detecting buried landmines," *IEEE Trans. Antennas Propagat.*, Vol. 46, 1419–1426, Oct. 1998.
9. Zainud-Deen, S. H., M. E. Badr, K. H. Awadalla, and H. A. Sharshar, "Microstrip antenna for detecting buried landmines," *23rd NRSC2006 Symp.*, Faculty of Electronic Engineering, Menoufya, Univ. Menouf, Egypt, Mar. 2006.
10. Zainud-Deen, S. H., M. E. Badr, K. H. Awadalla, and H. A. Sharshar, "Microstrip antenna with shorting pins as a sensor for landmines detecting," *24th NRSC2007 Symp.*, Faculty of Engineering, Ain Shams Univ., Cairo, Egypt, Mar. 2007.
11. Zainud-Deen, S. H.. M. E. Badr, E. El-Deen, K. H. Awadalla, and H. A. Sharshar, "Microstrip antenna with corrugated ground plane surface as a sensor for landmines detection," *Progress In Electromagentics Research B*, Vol. 2, 259–278, 2008.
12. Zainud-Deen, S. H., M. E. Badr, E. El-Deen, K. H. Awadalla, and H. A. Sharshar, "Microstrip antenna with defected ground plane structure as a sensor for landmines detection," *Progress In Electromagentics Research B*, Vol. 4, 27–39, 2008.
13. Yee, K. S., "Numerical solution of initial boundary value problems involving Maxwell's equations in isotropic media," *IEEE Trans. Antennas Propagat.*, Vol. 14, 302–307, 1966.
14. Taflove, A., *Computational Electrodynamics: The Finite Difference Time Domain Method*, 2nd edition, Artech House, Norwood, MA, 2005.
15. Ali, E. M., "Analysis of electromagnetic waves in the time domain," M.Sc. Thesis, Faculty of Electronic Engineering, Menoufia Univ., Menouf, Egypt, 2006.